

International Conference on Space Optics—ICSO 2014

La Caleta, Tenerife, Canary Islands

7–10 October 2014

Edited by Zoran Sodnik, Bruno Cugny, and Nikos Karafolas



Small facility for linear variable filter characterization

P. Blain

N. Ninane

V. Moreau

Y. Stockman



icso proceedings



SMALL FACILITY FOR LINEAR VARIABLE FILTER CHARACTERIZATION

P. Blain¹, N. Ninane¹, V. Moreau² and Y. Stockman¹

¹CSL, Spatial Center of Liège, University of Liège, Avenue du Pré Aily, Liège, Belgium;

²AMOS, Advanced Mechanical and Optical Systems, rue des Chasseurs Ardennais, 2, Liège, Belgium;

I. INTRODUCTION

The use of Linear Variable Filters (LVFs) has already been proposed as an alternative to other dispersion elements for imaging spectroscopy [1]. The major advantage of these filters is their compactness. Basically, one filter put in front of an array detector allows recording a hyper spectral image in push-broom mode, which is a relatively inexpensive and compact design.

Variable linear filter consists in an interference coating with variable thickness, such that the transmitted wavelength varies linearly along the filter versus the position on the filter as shown in fig.1.

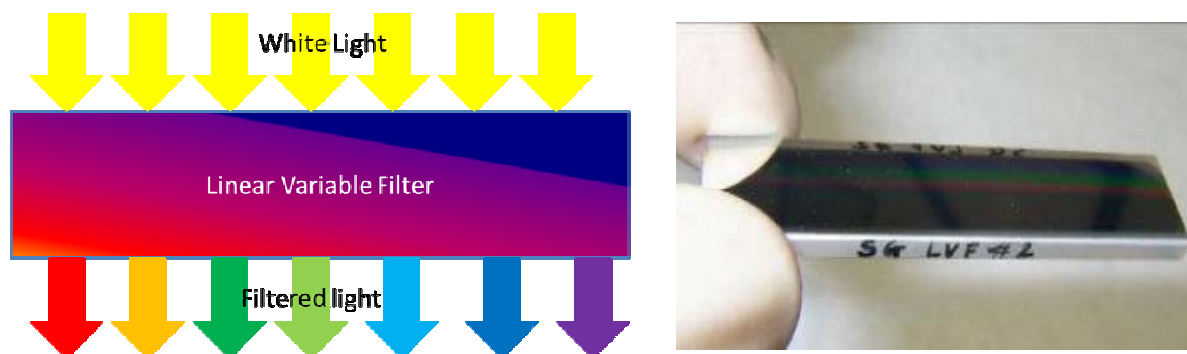


Fig. 1. Principle of Linear Variable Filter (left). Picture of a LVF [courtesy of AMOS s.a.] (right).

An independent setup is implemented using a board level camera, a monochromator and lenses. This kind of set-up has already been used by LVF manufacturers for characterizing their filters. A lens placed after the monochromator ensures a collimated beam impinging the LVF. Using this technique a mean bandwidth of 10 nm is claimed.

The approach presented here is slightly different. Instead of using a collimated beam, a set-up with a converging beam impinging on the LVF is developed. The purpose of that change is to match the telescope f-number in which the spectral instrument could be used.

This paper aims to describe the major steps of the work performed at CSL (Spatial Center of Liège) to develop a small facility to characterize LVFs. The paper describes first the characteristics of interests for such optical elements, and then presents the set-up. Results that prove the usefulness of the facility are finally demonstrated.

II. PROPERTIES OF LVF

The spectral system is composed of two elements, a detector (usually a matrix detector) and the filter itself placed as close as possible to the detector. In order to facilitate the interpretation of the signal, the spectral lines are put parallel to the matrix detectors lines. Nevertheless this is not always perfect (for several reason presented here after); this default is called spectral registration error.

LVFs are characterized by their spectral registration which is the spectral equation for the correspondence between the line of the CMOS sensor and the wavelength that passes the LVF.

Another parameter is the spectral resolution characterized by the full bandwidth at half maximum (FWHM). The FWHM of a pulse is the distance between two points of abscissa whose ordinate is equal to half the maximum. One can interpret the FWHM as the minimum distance necessary to distinguish unmistakably two distinct wavelengths.

A last parameter to characterize is the spectral rejection, i.e. the rejection ratio between the useful signal and the noise for one recorded line.

In theory, each line of the LVF is straight and parallel to the edges of the filter (cf. fig.2). However, in reality, a line of LVF is parabolic (smile) and is not parallel to the edge of LVF.

When at a given wavelength, the light strip on the CMOS is not perfectly straight. There are 3 deformations which modify the light strip: the tilt, the smile and the sinusoid.

- The tilt (in pixels) of a line with respect to a LVF CMOS line. The total tilt is the sum of two tilts:
- Alignment Tilt: CMOS and LVF are not perfectly parallel. Thus, a LVF line and a CMOS line are not perfectly parallel.
- Manufacturing Tilt: a line of LVF is never perfectly parallel to its edges. This tilt is an inherent to manufacturing process and can be corrected during post processing.
- Due to the manufacturing process, the lines of LVF are not straight; they are slightly parabolic. We call this deformation smile.

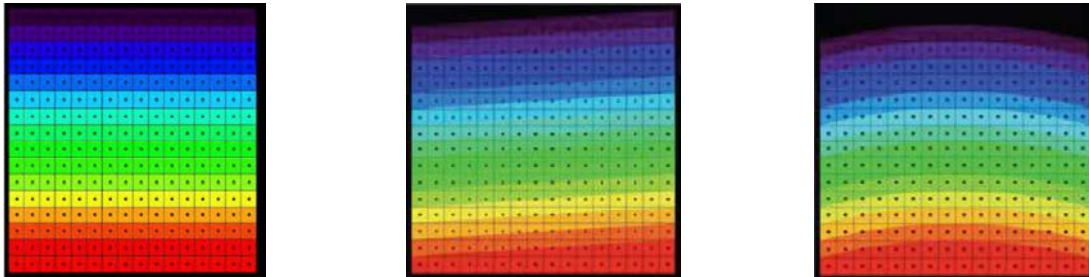


Fig. 2. Ideal LVF (left). Tilted LVF (center). LVF with a smile (right).

III. EXPERIMENTAL SET-UP

The different elements of the set-up are:

- A 300 Watt Xenon lamp from Oriel
- A Newport MS-257 monochromator. Allows selecting bandwidth smaller than the LVF one.
- A 18.8 cm integrating sphere ensures spatial uniformity of the beam and its non-polarized state.
- 2 lenses ($f_1 = 98\text{mm}$ and $f_2 = 150\text{mm}$)
- An OEM CMOS sensor from PixelLink (the lens tube was removed so the LVF can be stuck as close as possible to the CMOS chip, an IR filter window remains in front of the CMOS chip.
- A LVF is placed on a mount so that its height can be controlled via a micrometric stage. Thus one can change the wavelength range to be seen on the CMOS sensor.



Fig.3. Picture of the small facility.

III. DATA PROCESSING

The monochromator bandwidth is set at 2.8 nm. This value is a compromise between the intensity of the input flux and a narrow bandwidth (more than 3 times less than the required LVF bandwidth). Pictures with and without the LVF are recorded for each wavelength. The transmission of the LVF is given by their ratio. In order to minimize Gaussian noise, several pictures are taken and a mean is computed. A DC component (recorded

with the lamp off) is subtracted to suppress non Gaussian noise. Pictures of 1280 lines by 1024 columns are recorded.

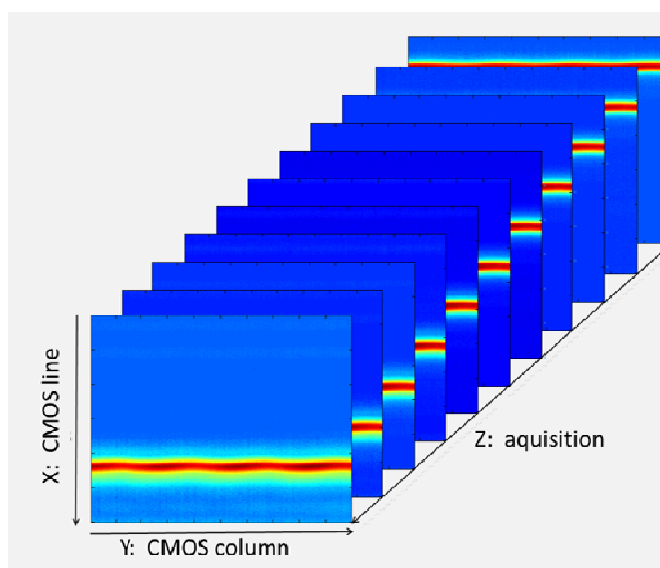


Fig. 4. LVF transmission cube

The recording of the data leads to a transmission cube with transmission lines for each wavelength (cf. Fig.4). It is possible to reduce the size of the cube to the one of a 2D matrix, by meaning the cube along its columns. This matrix is called the LVF matrix (cf. Fig.5). This matrix is easier to process.

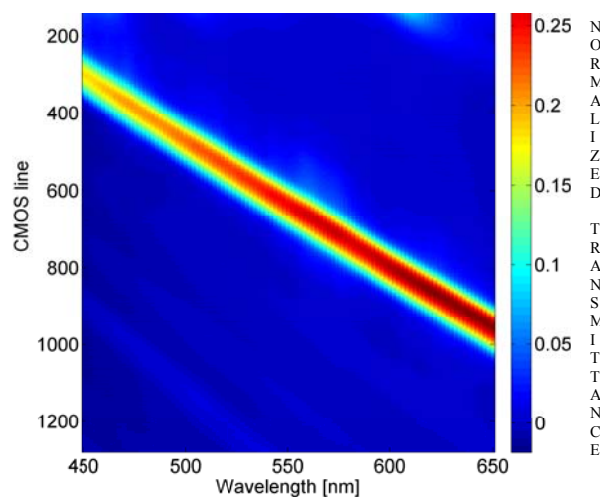


Fig. 5. Normalized transmittance given by the LVF matrix between 450 and 650 nm with a 2 nm step.

III. RESULTS

A. Spectral registration

For each wavelength, the maximum for each column of the LVF matrix are taken into account. A pixel position is associated to a wavelength. The obtained curve is then interpolated with a one degree polynomial. The following equation was obtained with a correlation coefficient of 0.9998.

$$\lambda_s = 0.282 \cdot x + 402.6639 \quad (1)$$

A second degree polynomial fitting was also tried and allowed a 0.9999 correlation coefficient. But the compromise between time computation and gain in precision lead us to choose the one degree polynomial fitting.

B. Measured FWHM

The FWHM is computed along the CMOS line. As one can see on fig.6, the first lines (from 0 to 300) and the last ones (1000 to 1280) are not relevant for the FWHM calculation because there is no useful signal within them. They are thus ignored. The Mean computed FWHM is 13.6 nm. The error is about +/- 1 nm.

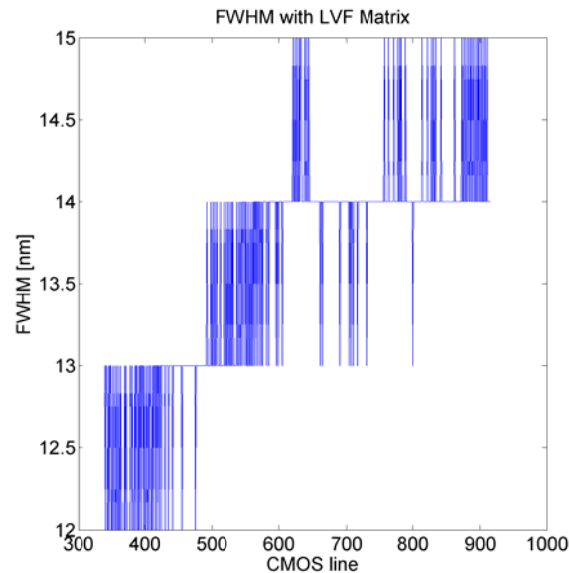


Fig. 6. FWHM calculation across the lines of the detector for wavelength between 450 and 650 nm.

The wavelength range can be extended to 900 nm by translating the LVF vertically with the micrometric translation stage. The sensor allows recording a range of 300 nm. A LVF matrix from 600 nm to 900 nm is computed. The Mean computed FWHM is 17.2 nm. With the set-up the FWHM varies versus the wavelength.

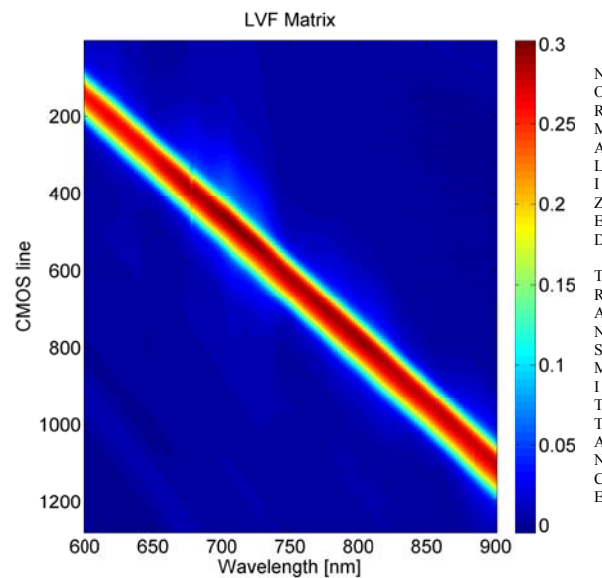


Fig.7. Normalized transmittance given by the LVF matrix between 600 and 900 nm with a 2 nm step

C. Influence of the f-number

The measured FWHM are different that those claimed by the manufacturer. The influence of the divergence of the input beam is thus measured. The measurement was made at a wavelength of 650 nm. An iris diaphragm is

set at the output of the integrating sphere (a 1 inch diameter output). The aperture of the iris is reduced ($f/5$ to $f/4$) in order to reduce external angles. A measurement is even made while removing L2 so that a collimated beam is impinging the CMOS chip.

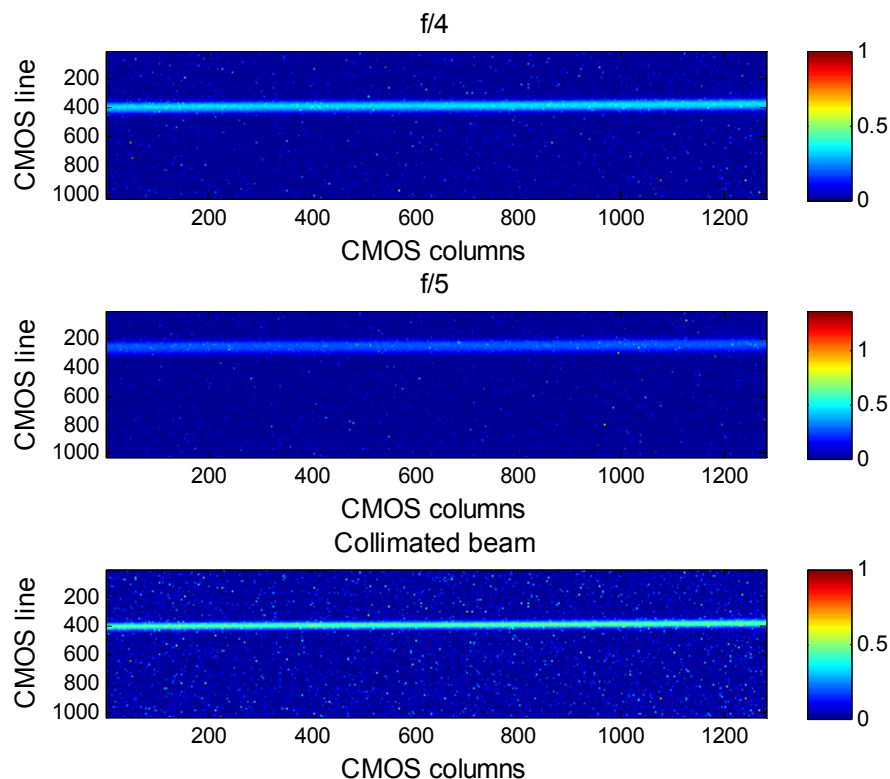


Fig.8. Transmission maps for different divergence f-numbers at 650 nm. From top to bottom: $f/4$, $f/5$ and collimated beam.

The integration time still remains 1000 ms. As closing the iris aperture reduces the amount of incoming light, the noise and measurement uncertainty increase (cf. fig.8). Thus the images are filtered out by use of 5×5 average filters.

The FWHM increases with the aperture size (cf. Table 1). The use of a collimated beam is representative of the LVF characteristics. But it is not representative of the case when it is used in a telescope setup. The experiment showed the influence of the aperture size on the FWHM, and as expected the FWHM increases with the $F/\#$ since the range of incident angle on the filter increases.

Table.1. Evolution of the measured FWHM with respect to the f-number

| FWHM | $f/5$ | $f/4$ | Collimated beam |
|-----------|---------|--------|-----------------|
| Mean (nm) | 14.5003 | 17 | 9.4985 |
| Std (nm) | 2.0264 | 4.0102 | 1.0462 |

D. Influence of the polarization state

A rotating polarizer is placed after the lenses. Only three wavelengths are used (550, 650 and 750 nm). A measurement is made every 5 arcdegrees. The intensity maps represent a mean along columns of each averaged pictures. An average picture is computed from the mean of 10 acquisitions with the same integration time and including dark subtracting. Each column of the intensity map corresponds to a polarization orientation. Transmission maps are also computed, an example is given in fig.9.

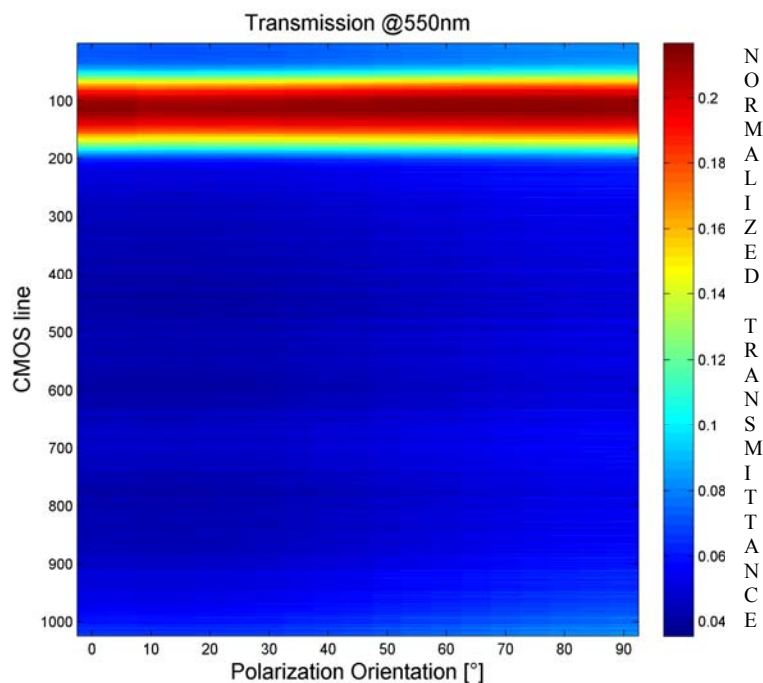


Fig.9. Transmission at 550 nm for different orientation of polarization.

The transmission maps should then give an idea of the LVF influence on polarization. Transmission maps (cf. Fig.9) show no obvious variation.

Table 2 sums up the polarization variation for several wavelengths and also gives an overview of the noise sources within the measurements.

Table.2. Transmission and noise evaluation

| | 550 nm | 650 nm | 750 nm |
|------------------------|-------------|---------|---------|
| Transmission peak | 0.2157 | 0.2294 | 0.2531 |
| STD transmission peak | 9.1813e-004 | 0.0011 | 0.0014 |
| Read out noise | 0.0059 | 0.0059 | 0.0059 |
| Thermal noise | Removed | Removed | Removed |
| Shot noise (3std/mean) | 0.0128 | 0.0144 | 0.0166 |
| Overall noise | 0.0187 | 0.0203 | 0.0225 |

The non-sensitivity to input polarization state has been demonstrated, confirming that LVF could be used without being affected by polarization compared to most grating based set-ups.

V. CONCLUSION

The presented facility allows evaluating LVF and fully characterizing them in terms of registration, resolution, rejection and polarization. By matching the f-number of the set-up in which the LVF is foreseen, one can see what will be its impact on the spectral performance of the spectro imageur.

ACKNOWLEDGEMENT

The authors are grateful to the Région Wallonne Government which subsidized this research via the ACTIO Plan Marshall project.

REFERENCES

- [1] M. Taccola, S. Grabarnik, L. Maresi, V. Moreau, L. de Vos, Y. Versluys, G. Gubbels, "Compact Multispectral and Hyperspectral Imagers based on a Wide Field of View TMA", ISCO, Rhodes, October 4, 2010.